

Magnetic resonance microscopy and micro computed tomography of brain phenotypes of two FGFR2 mouse models for Apert syndrome.

T. Neuberger¹, K. Aldridge², C. A. Hill², J. A. Austin², T. M. Ryan³, C. Percival³, N. Martinez-Abadias³, Y. Wang⁴, E. Wang Jabs⁴, A. G. Webb^{5,6}, and J. T. Richtsmeier³

¹The Huck Institutes of the Life Sciences, Pennsylvania State University, University Park, PA, United States, ²University of Missouri-School of Medicine, ³Department of Anthropology, Pennsylvania State University, University Park, PA, United States, ⁴Department of Genetics and Genomic Sciences, Mount Sinai School of Medicine, ⁵Department of Bioengineering, Pennsylvania State University, University Park, PA, United States, ⁶Department of Radiology, Leiden University Medical Centre, Leiden, Netherlands

Introduction. Apert syndrome (AS) is one of a number of genetic syndromes associated with craniosynostosis, occurring in 1 in 12.4-15.5/million live births [1,2], with 99% of cases associated with one of two missense mutations in adjacent amino acids, Ser252Trp and Pro253Arg, of fibroblast growth factor receptor 2 (FGFR2). Individuals with AS display what has been described as a stereotypical constellation of dysmorphologies, most often including craniofacial dysmorphism and central nervous system (CNS) anomalies. The relative severity of brain dysmorphism and cognitive effects varies widely among individuals with AS [3, 4]. The nature of the association between phenotypic abnormalities and cognitive deficits is not known, but it has been shown that early surgical treatment of cranial dysmorphologies does not prevent mental deficiencies [5]. Due to the wide diversity of brain phenotypes among individuals of AS, their low numbers, and a possible environmental effect during growth the variation in brain phenotypes in AS cannot be studied in humans. Hence, this work compares two AS genetic mouse mutations the Apert syndrome $Fgfr2^{+/S252W}$ mouse [6] and the Apert syndrome $Fgfr2^{+/P253R}$ mouse (Sun et al. submitted) to their wildtype litter mates at P0 using three dimensional magnetic resonance microscopy (MRM). Cranial suture fusion was assessed by using micro computed tomography (μ -CT).

Materials and Methods. The Apert $Fgfr2^{+/S252W}$ (n = 8) and $Fgfr2^{+/P253R}$ (n = 14) and the wildtype (n = 11) mice were sacrificed, weighed, and fixed in 4% paraformaldehyde. To reduce the MR scanning time the animals were immersed in a 2% Magnevist (Bayer Health Care, Wayne, NJ) phosphor-buffered solution for ten days. The achieved short T1 (32 ms) and T2 (8 ms) times allowed for fast imaging with a high contrast-to-noise ratio. To prevent the brains from drying out and to minimize magnetic susceptibility artifacts during scanning the specimens were surrounded by a fluorinert liquid FD-43 (3M, St. Paul, MN). All experiments were conducted on a vertical 14.1 tesla Varian (Varian Inc., Palo Alto, CA) imaging system with direct drive technology. A home-built loop gap resonator with a diameter of 2.0 cm was used to acquire three-dimensional spin echo images of the head of the animal. Images up to an isotropic resolution of 40 μ m were acquired. A standard imaging experiment with an isotropic resolution of 80 μ m comprised a field of view of 15.4 x 14 x 11 mm³ and a matrix size of 192 x 132 (75% partial Fourier) x 137. With eight averages and a repetition time of 75 ms (echo time 25 ms) the total scan time was three hours. Matlab (The MathWorks, Inc., Natick, MA) was used for post-processing. By zero-filling each direction by a factor-of-two the pixel resolution of the standard imaging experiment was 40 μ m³. Micro-computed tomography (μ -CT) images were acquired using a HD-600 OMNI-X high-resolution X-ray computed tomography system (Bio-Imaging Research Inc, Lincolnshire, IL) following already established protocols [7] with pixel size of 0.15-0.02 mm and 0.15-0.025 slice thickness.

Results. MRM images were reconstructed in 3D to visualize and assess the gross morphology of the brain. All non-neural tissues (e.g. skull, dura, blood vessels), as well as the olfactory bulbs were removed from the MRM images using Analyze 9.0® [8] in order to reconstruct the brain surface. From these reconstructions, we assessed overall brain morphology, brain symmetry, gross defects of the corpus callosum, and ventriculomegaly of the lateral ventricles and 4th ventricle. Example phenotypes are illustrated in Figure 1. At P0 no increase in brain size between the two mutations and the wild type mice were observed. In $Fgfr2^{+/S252W}$ mice, the most frequently observed anomaly is asymmetry of cerebral hemispheres, while only two of the $Fgfr2^{+/P253R}$ mice showed asymmetry. However, the presence and the severity of cerebral asymmetry do not correlate with the pattern of coronal suture fusion when compared to the μ -CT data. Two of the $Fgfr2^{+/S252W}$ and three $Fgfr2^{+/P253R}$ mice in this study show an arched or rounded corpus callosum (Figure 3) on the midsagittal plane. This number is similar to the ~30% observed in humans [5]. Ventriculomegaly is often observed in humans with AS [5, 9]. In our study only one of the mice displayed larger lateral ventricles ($Fgfr2^{+/P253R}$), though three mice were observed to have enlarged 4th ventricles (two $Fgfr2^{+/S252W}$ and one $Fgfr2^{+/P253R}$). Further investigation of this trait is necessary to determine the cause for the divergent findings.

Conclusion. By using MRM we have demonstrated anomalies of the developing brain in two $Fgfr2$ models for Apert syndrome. Our data suggest little or no relationship between patterns of suture closure and brain dysmorphism at P0 when compared to the μ -CT data. Continuing analysis of the co-development of these two tissues will further define change in local developmental processes that underlie craniosynostosis phenotypes and their variation. Further dissection of the production of skull and brain morphology, and the developmental relationships between these two important tissues, are necessary to elucidate the genotype-phenotype continuum in craniosynostosis.

References. [1]. Cohen M et al. Am J Med Genet 42:655-659, 1992. [2] Tolarova M et al. Am J Med Genet 72:394-398, 1997. [3] Blank C et al. Ann Hum Genet Lond 24:151-164,1960. [4] Renier D et al. J Neurosurg 85:66-72. 1996. [5] Cohen M et al. Am J Med Genet 35:36-45, 1990. [6] Wang Y et al. Development 132:3537-48, 2005. [7] Parsons T et al. Anat Rec 290:414-421, 2007. [8] Robb RA et al. Comput Med Imaging Graph 13:433-454, 1989. [9] Noetzel M et al. J Pediatr 107:885-892, 1985.

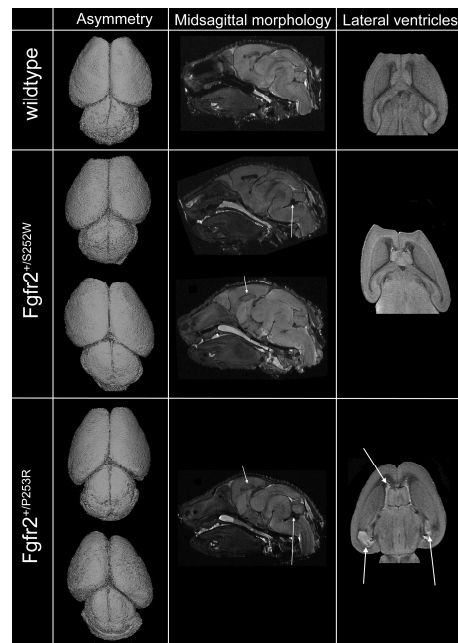


Figure 1: Three-dimensional reconstructions of superior surfaces (1st column), midsagittal planes (2nd column), and axial slice images (last column) of MRM data, illustrating examples of variation in brain phenotypes. Row 1: wildtype mouse. Row 2: $Fgfr2^{+/S252W}$ mice with slight cerebral asymmetry (above) and severe cerebral asymmetry (below), enlarged 4th ventricle (above, white arrow) and arched corpus callosum (below, white arrow), and unremarkable lateral ventricles. Row 3: $Fgfr2^{+/P253R}$ mice with slight cerebral asymmetry (above) and severe cerebral asymmetry (below), enlarged 4th ventricle and arched corpus callosum (white arrows) and enlarged lateral ventricles (white arrows).